

基于超声振动的 304 不锈钢 TIG 焊接

范阳阳， 孙清洁， 杨春利， 林三宝<sup>\*</sup>  
(哈尔滨工业大学 现代焊接生产技术国家重点实验室, 哈尔滨 150001)

**摘 要:** 304 不锈钢是应用最为广泛的一种奥氏体不锈钢, 它具有优良的耐蚀性和耐热性, 优良的低温强度和力学性能. 304 不锈钢常用的焊接方法为 TIG 焊接. 普通 TIG 焊接由于焊缝熔深浅、焊接速度低、焊接效率较低, 而且在焊接过程中容易出现焊缝区和热影响区的晶粒粗大, 造成焊接接头质量下降. 功率超声振动是金属凝固过程中改善组织、提高力学性能的有效方法之一. 为了提高焊接效率和改进接头的质量, 将超声振动通过机械耦合方式引入 304 不锈钢 TIG 焊接的过程中, 进行了平板堆焊试验. 结果表明, 施加超声后焊接的熔深有效增加, 深宽比增大, 焊缝结晶方式由粗大柱状晶转变为细小的树枝晶和等轴晶, 晶粒度减小, 熔合区组织均匀化.

**关键词:** 超声; 细化晶粒; 组织均匀

中图分类号: TG115. 28 文献标识码: A 文章编号: 0253—360X(2009)02— 0091— 04



范阳阳

0 序 言

304 不锈钢是应用最为广泛的一种奥氏体不锈钢, 它具有优良的耐蚀性和耐热性, 优良的低温强度和力学性能, 而且由于成分是单相奥氏体组织, 无热处理硬化现象, 广泛应用于建筑、汽车、化学工业、船舶制造等行业. 304 不锈钢常用的焊接方法为 TIG 焊接. 普通 TIG 焊接由于焊缝熔深浅、焊接速度低、焊接效率较低<sup>[1]</sup>, 而且在焊接过程中容易出现焊缝区和热影响区的晶粒粗大, 造成焊接接头质量下降, 通常达不到设计使用寿命就报废. 如何提高焊接效率和改进接头的质量一直是研究的热点.

功率超声振动是金属凝固过程中改善组织、提高力学性能的有效方法之一, 最早被应用在铸造技术中<sup>[2]</sup>. 功率超声波在液态金属中传播时, 其高频振动和辐射压力对媒介产生机械作用、热作用、空化作用和声流作用等, 对液态金属结晶过程造成影响, 其公认的效果有细化晶粒、组织均匀化、组织净化(去气、除渣、提纯等). 目前这种方法已经在铸造行业中得到了广泛应用<sup>[3]</sup>, 但是在电弧焊接中应用较少, 主要通过在工作件上施加功率振动来对熔池凝固过程产生作用<sup>[4, 5]</sup>, 而通过焊枪向熔池施加超声振动尚未有报道. 文中通过焊枪向熔池施加超声振

动, 研究超声对焊接过程的影响, 为超声振动在电弧焊接中的进一步研究奠定基础.

1 试验方法

试验系统原理如图 1 所示. 试验所使用功率超声系统为自行设计, 包括超声波发生器和超声振动系统, 最大工作功率为 600 W. 焊接电源为德国 LORCH 公司生产的 V24 型 TIG 电源, 最大焊接电流为 240 A. 通过机械耦合装置将超声波施加到焊枪上. 超声经过 TIG 焊枪端部和电弧后传播到熔池中, 对熔池液态金属作用, 改变熔池的结晶凝固过程.

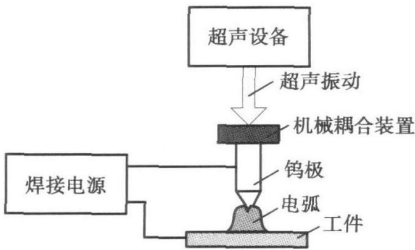


图 1 试验系统原理图  
Fig. 1 Schematic of experimental system

堆焊。在相同的工艺下,分别考察施加超声后 TIG 焊接和普通 TIG 焊接两种情况下 304 不锈钢焊缝尺寸及微观组织变化。所使用的焊接工艺参数如表 2 所示。为了保证试验结果的准确性,在每条焊缝焊接之前,重新研磨电极呈标准形状,调整电弧至标准长度,保证每条焊缝均在同一工艺下焊接。

表 1 304 不锈钢化学成分(质量分数,%)  
Table 1 Chemical composition of 304 stainless steel

C	S	P	Si	Mn	Cr	Ni	N	Fe
0.08	0.03	0.045	0.75	2	18~20	8~10.5	0.1	余量

表 2 焊接工艺参数  
Table 2 Welding parameters

焊接 电流 $I/A$	焊接 速度 $v/(mm\cdot min^{-1})$	保护气 流量 $q/(L\cdot min^{-1})$	电弧 长度 $l/mm$	钨极 直径 $d/mm$	钨极 角度 $\theta/(^{\circ})$
150	120	12	4	3.2	60

焊前对试样进行清理,利用钢丝刷和丙酮清理

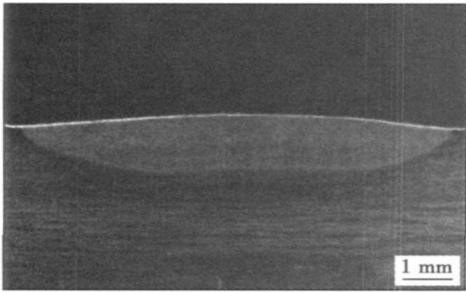
板材表面的水、油污、氧化膜等杂质,保证焊接过程稳定。在施加超声进行焊接前,调节超声设备为谐振状态,使焊枪电极端部超声振幅最大。焊后测量其表面熔宽和相同截面处的熔深,并利用金相分析方法分析试样的微观组织。

2 试验结果

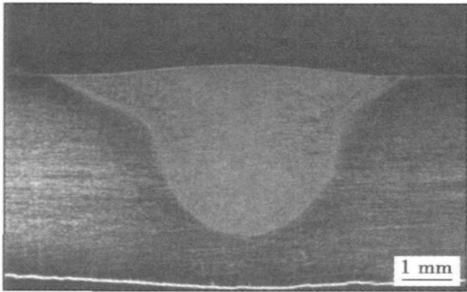
2.1 焊缝宏观形貌

在表 2 所示的工艺参数下进行了普通 TIG 焊接和在焊枪上施加超声 TIG 焊接。图 2 为普通 TIG 焊和施加超声 TIG 焊的焊道横截面形貌。

焊缝的形状尺寸与焊缝的力学性能有着直接的关系,而且会影响熔池中气体逸出的难易、熔池的结晶方向、成分偏析、裂纹倾向性等<sup>[1]</sup>。考察超声对焊缝形状尺寸带来的变化具有重要意义。在图 2 所示的焊缝断面宏观形貌中测量普通 TIG 焊和施加超声 TIG 焊的焊缝尺寸,如表 3 所示。结果表明,在施加超声振动后,焊缝熔深增加了 214%,熔宽减小了 18%,深宽比大幅度增加。



(a) 普通TIG焊



(b) 施加超声后TIG焊

图 2 焊缝横截面宏观形貌

Fig. 2 Macroscopical appearances of weld cross-section

表 3 焊缝形状尺寸  
Table 3 Dimensions of weld shape

	熔深 $H/mm$	熔宽 $B/mm$	余高 $a/mm$	深宽比
普通 TIG 焊	1.18	8.5	0.25	0.14
超声 TIG 焊	3.71	6.93	0.27	0.54

2.2 焊缝微观组织

304 奥氏体不锈钢板焊缝的金相组织为奥氏体和奥氏体基体上分布的  $\delta$  铁素体。在 304 不锈钢焊接中,焊缝中希望含有体积分数为 5%~10% 的  $\delta$  铁素体,形成  $\gamma+\delta$  的双相焊缝组织。这是因为焊缝中有一定的  $\delta$  相可以细化晶粒,打乱奥氏体粗大柱

状晶的方向性,提高焊缝屈服强度,而且  $\delta$  铁素体可以改善晶界两边的贫铬现象,防止晶间腐蚀。

在焊枪上施加超声振动前后焊缝底部低倍显微组织见图 3。图 3 中,普通 TIG 焊缝中,可以看到明显的垂直于熔合线方向生长的粗大柱状晶,柱状晶由于过热严重长大,一直长到焊缝中心附近,只有在焊缝中心靠近表面的一小块区域内存在着少量等轴晶。当在焊枪上施加超声后,焊缝的结晶方式由粗大的柱状晶为主转化为细小的树枝晶和等轴晶为主,此结果可以通过奥氏体边界上的  $\delta$  铁素体的分布说明。

在柱状晶区,当沿不同方向生长的两组柱状晶相遇时,会形成柱状晶晶界。柱状晶晶界是杂质、气泡、缩孔较富集的地区,易于沿晶界形成裂纹,成为

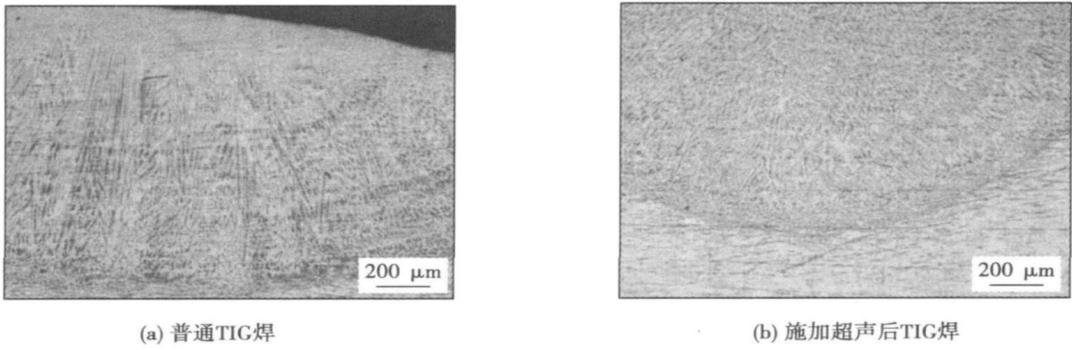


图 3 焊缝底部微观组织  
Fig. 3 Microstructures of the bottom of weld

焊缝的薄弱地带<sup>[6]</sup>. 与柱状晶区相比, 细小的树枝晶和等轴晶区的各个晶粒在长大时彼此交叉, 枝叉间的搭接牢固, 裂纹不易扩展, 不存在明显的脆弱界面; 各晶粒取向不尽相同, 其性能也没有方向性, 因而在焊接时都期望得到细小的树枝晶和等轴晶. 从这个角度来看, 超声 TIG 焊能够大幅提高焊缝等轴

晶所占的比例, 提高焊缝的力学性能和抗裂性能. 选取图 3 中具有典型晶粒特征的区域进行显微放大, 普通 TIG 焊和施加超声后 TIG 焊的焊缝粗晶区和熔合区的显微组织对比图见图 4 和图 5. 图 4 中, 当焊枪上施加超声振动后, 焊缝粗晶区的晶粒产生了明显的细化,  $\delta$ 铁素体的分布更细小均匀.

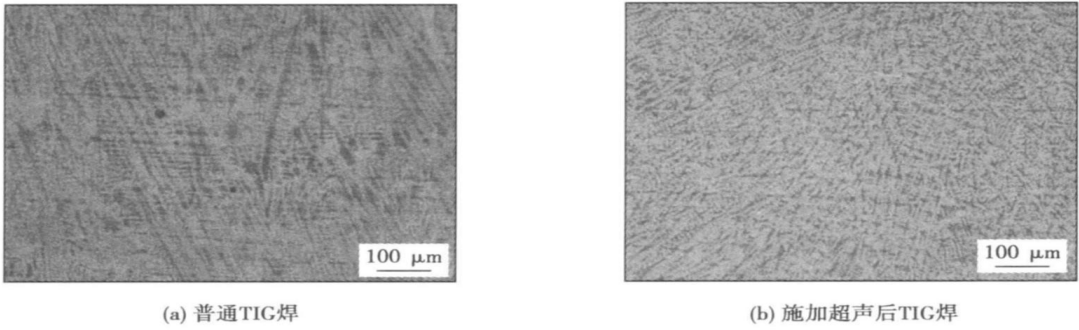


图 4 焊缝粗晶区微观组织  
Fig. 4 Microstructures of coarse grain zone

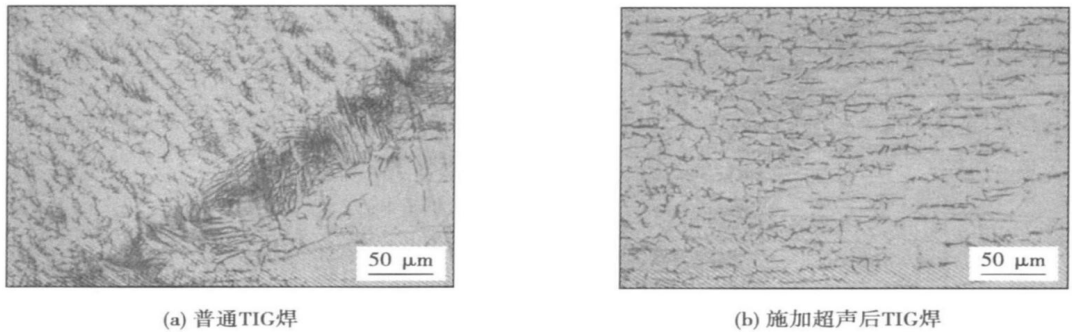


图 5 焊缝熔合区微观组织  
Fig. 5 Microstructures of weld bond

在图 5 所示熔合区, 超声振动的引入使熔合区的组织均匀化. 普通 TIG 焊焊缝熔合线上散乱分布

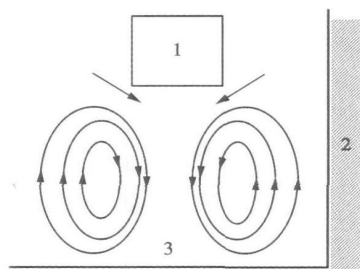
着大量失去枝晶特征的  $\delta$ 铁素体, 而在施加超声后焊缝熔合线上  $\delta$ 铁素体分布比较均匀.

从试验结果可以证明,在焊枪上施加超声不但改变了焊缝形状尺寸,而且对焊缝区的晶粒细化和组织均匀化有明显的效果。

### 3 讨 论

在施加超声后 TIG 焊接过程中,超声振动被引入到熔池中。超声波在熔池中传播时,会对熔池液态金属产生交变振动作用、力作用和空化作用等相互作用,给熔池带来机械搅拌、相互扩散、热效应、空化效应和声流效应等超声效应,影响熔池内部金属流动和结晶过程。

对于施加超声后 TIG 焊焊缝熔深增加,深宽比增大的原因,主要是超声的热作用、声流作用带来的影响。在超声传播过程中,由于液态金属的粘滞性,一部分声能被液体吸收并转化为热能,导致熔池金属温度的升高。同时,这种吸收导致超声振幅的有限衰减,在熔池内形成了从上至下的声压梯度,导致液体流动。当声压超过一定值时,液体中可以产生一个流体的喷射,这就是声流<sup>[7]</sup>,如图 6 所示。声流的速度比质点振动速度小很多,但亦能达到流体热对流速度的 5~10 倍。在声流效应的作用下,温度更高的液态金属高速向熔池底部流动,从而形成了更大的熔深。



1. 超声源; 2. 凝固前沿; 3. 熔体

图 6 声流效应示意图

Fig. 6 Schematic of acoustic streaming

施加超声后,熔池结晶形式由柱状晶为主转化为等轴晶为主,而且出现了晶粒细化现象和组织均匀现象。结合金属凝固理论和超声理论进行分析,认为是由于机械搅拌、相互扩散、声流效应等超声效应带来了熔池内部金属的强烈对流,这种对流会将很多正在结晶长大的晶粒打碎,抑制晶粒的生长,也形成了大量的可作为晶核的残枝碎片。同时,这种对流将熔池上部的高温金属液带到熔池底部,使整个熔池区域的液态金属温度趋于一致。这样,在整

个熔池的中心区域形成了更有利于等轴晶形核生长的条件,使熔池结晶形式发生了由粗大柱状晶到细树枝晶和等轴晶的转变。同时,熔池中存在着许多微小的气泡,这为空化效应的产生创造了条件。空化泡在闭合瞬间会产生激波,形成局部的高温高压和冲击波,这种冲击波的能量足以将正在形成的晶粒破碎成几个小块,进而达到细化晶粒的目的。

### 4 结 论

(1) 在焊枪上施加超声振动后,304 不锈钢焊缝的熔深增加,深宽比加大。

(2) 通过金相观察发现,施加超声振动焊接后,304 不锈钢焊缝的晶粒细化,组织更均匀。

(3) 超声的热效应、声流效应和空化效应引起的熔池温升和热对流是熔深增加的主要原因;超声机械效应、声流效应引起的熔池对流和空化效应引起的冲击波是显著细化焊缝晶粒、均匀化组织的主要原因。

### 参考文献:

- [1] 杨春利,林三宝.电弧焊基础[M].哈尔滨:哈尔滨工业大学出版社,2003.
- [2] 马立群,舒光翼,陈 锋.金属熔体在超声场中凝固的研究[J].材料科学与工程,1995,13(4):2-6.  
Ma Liqun, Shu Guangji, Chen Feng. Research on solidification of metal melt under ultrasonic field [J]. Materials Science And Engineering, 1995, 13(4): 2-6.
- [3] 郭 峰,罗沛兰,毕 丘,等.金属熔体超声细化处理技术的研究进展[J].金属材料与冶金工程,2008,36(1):59-64.  
Guo Feng, Luo Peilan, Bi Qiu, et al. Review on metal melt treatment technology using with ultrasonic field [J]. Metal Materials and Metallurgy Engineering, 2008, 36(1): 59-64.
- [4] Cui Y, Xu C L, Han Q. Effect of ultrasonic vibration on unmixed zone formation [J]. Scripta Materialia, 2006, 55(11): 975-978.
- [5] Dai Wendong. Effects of high-intensity ultrasonic-wave emission on the weldability of aluminum alloy 7075-T6 [J]. Materials Letters, 2003, 57(16-17): 2447-2454.
- [6] 崔忠圻,刘北兴.金属学与热处理原理[M].哈尔滨:哈尔滨工业大学出版社,1998.
- [7] 马大猷.高声强: I. 基础[J].声学学报,1992,17(4):241-247.  
MAA Dahyou. High-intensity sound: I. Fundamentals [J]. Acta Acustica, 1992, 17(4): 241-247.

作者简介:范阳阳,男,1985 年出生,博士研究生,研究方向为高效化焊接。发表论文 2 篇。

Email: fyangyang1985@163.com

**Key words:** magnesium alloy; hybrid welding; microstructure; mechanical properties

### Effects of peak temperature of welding thermal circle on hardness of 10CrMo910

LI Haitao, CHEN Fuqiong, HU Yanhua, XIE Ruijun (College of Materials Science and Engineering, Inner Mongolia University of Technology, Hohhot 010051, China). p75—78

**Abstract:** With the welding heat-cycle system which voluntarily design, through measuring temperature signal in real-time tests on different positions of two welded joints under the different welding parameters. The effects of peak temperature of welding thermal circle on hardness of 10CrMo910 have been researched. The test result indicated that welding heat-cycle has a greater influence on the value of hardness, when the peak value temperature is lower than 1 150 °C, hardness value increases with the peak value temperature increasing when the peak value temperature is higher than 1 150 °C, hardness value decreases with the peak value temperature increasing.

**Key words:** welding thermal circle; hardness; peak temperature

### Investigation on laser clad nano-Y<sub>2</sub>O<sub>3</sub> and cobalt based composite coating

YANG Shanglei<sup>1,2</sup>, ZHANG Wenhong<sup>3</sup>, LI Fabing<sup>1</sup>, HU Fengguang<sup>3</sup>, CHEN Aizhong<sup>3</sup>, LÜ Yunjiang<sup>3</sup> (1. College of Material Science and Engineering, Qingdao University of Science and Technology, Qingdao 266042, China; 2. Department of Mechanical Engineering, Tsinghua University, Beijing 100084, China; 3. Yankuang Luan Chemical Fertilizer Plant, Tengzhou 277527, China). p79—82

**Abstract:** A composite coating was prepared on a Ni-based alloy substrate by using laser cladding as well as surfacing welding with nano-Y<sub>2</sub>O<sub>3</sub> and Co-based alloy powders. The microstructure and microhardness of the nano-Y<sub>2</sub>O<sub>3</sub>/Co-based composite coating were investigated using various techniques, e. g., scanning electron microscope (SEM). The wear resistance property and corrosion resistance property of the nano-Y<sub>2</sub>O<sub>3</sub>/Co-based laser cladding composite coating and pure surfacing welding were analyzed by wear test and corrosion test. The results showed that the microstructure of laser cladding layer consists of a melt zone, a fine equiaxial zone and a coarse dendrite zone. The microhardness of the laser clad coating was measured as HV868. 9, superior to that of surfacing welding as HV512. 8. Furthermore the wear resistance of laser cladding coating is 51.2 times stronger, with a total wear value of 0.5 mg compared to 25.6 mg obtained from the surfacing welding. In the corrosion tests of 10% HCl, 10% HNO<sub>3</sub> or 10% NaOH solutions, the corrosion resistance properties of laser cladding coating is greatly enhanced.

**Key words:** nano-Y<sub>2</sub>O<sub>3</sub>; Co-based alloy; laser cladding

### Effect of activating fluxes on appearance of weld in thin plate electron beam welding of nickel-base super alloy GH4169

WANG Xichang, ZUO Congjin, CHAI Guoming, ZHANG Lianfeng (Beijing Aeronautical Manufacturing Technology Research Institute,

Beijing 100024, China). p83—86

**Abstract:** In this paper, the effects of different kinds of activating fluxes on appearance of weld was analysed during the electron beam welding (EBW) of nickel-base super alloy GH4169, oxides had deep influence on welding depth and weld formation of both sides of plate, while fluoride had no influence. And on base of it, activating fluxes which can greatly improve weld shape and surface quality of EBW are obtained by combination and optimization. The reason of improving appearance of weld is that, with activating fluxes change surface tension gradient in the weld pool, then affect the pattern of the fluid flow, consequently form narrow and deep, well shape weld. The results show that activating electron beam welding can improve appearance of weld and eliminate some surface defects such as undercutting, which is very useful during thin plate EBW.

**Key words:** activating electron beam welding; appearance of weld; surface tension gradient; weld pool flow pattern

### Numerical simulation on creep failure of dissimilar welded joint between martensitic heat-resistant steel and pearlitic heat-resistant steel

ZHANG Jianqiang, GUO Jialin, ZHANG Guodong, LUO Chuanhong, ZHANG Yinglin (School of Power and Mechanical Engineering, Wuhan University, Wuhan 430072, China). p87—90

**Abstract:** The maximum principal stress and Von Mises equivalent stress were simulated by FEM under the condition of 560 °C and applied stress level is 100 MPa, 120 MPa, 140 MPa respectively. The simulation results were validated with invariable stress accelerating test. The results show that the maximum principal stress is quite high in the vicinity of weld/12Cr1MoV interface for undematching weld joint, and creep cavities are easy to form in the weld/12Cr1MoV interface. With the increase of the acting stress, the maximum principal stress in the vicinity of weld/12Cr1MoV interface is increasing rapidly. However, the Von Mises equivalent stress is relatively low, and creep cavities are difficult of expansion. And only isolated cavities were found after accelerating test, early failure tendency is low. The stress concentrations of weld/12Cr1MoV interface is serious, the Von Mises equivalent stress is relatively high in the vicinity of weld/12Cr1MoV interface for overmatching weld joint, creep cavities are easy to form and expand. The creep damage and early failure tendency of overmatching weld joint are higher than those of undematching weld joint, and the interfacial creep rupture occurred after the accelerating test. Therefore, using undematching joint is reasonable for the dissimilar welded joint between martensitic and pearlitic steel.

**Key words:** martensitic heat-resistant steel; pearlitic heat-resistant steel; dissimilar metal welding joint; interfacial creep damage; numerical simulation

### TIG welding of the stainless steel 304 based on the ultrasonic vibration

FAN Yangyang, SUN Qingjie, YANG Chunli, LIN Sanbao, FAN Chenglei (State Key Laboratory of Advanced Welding Production Technology, Harbin Institute of Technology, Harbin 150001, China). p91—94

**Abstract:** Stainless steel 304 is one sort of the austenitic

stainless steel for most extensive use. It has excellent corrosion resisting and fire resisting property, high hypothermic strength and fine mechanical property. Its welding method is TIG in common use. The TIG welding method is an inefficient welding method because of its shallow penetration and low welding speed, the grain size of the weld is also inclined to grow up which may reduce the performance of the weld. Ultrasonic treatment is an effective way to minimize the grain size and improve the microstructure in the process of metal freezing. Ultrasonic treatment was lead in the process of TIG welding of stainless steel 304 to increase the welding efficiency and improve the weld property. Build-up welding experiments were taken on the flat plate. The results showed that the weld penetration and depth-to-width ratio increase and the crystallizing mode change from columnar crystals to small dendrite equiaxed crystals. Also, the grain size reduce and the organization of the fusion area is uniformed.

**Key words:** ultrasonic; grain refinement; uniform microstructure

**Thermal-mechano-metallurgical coupled analysis of welding residual stress** LIU Junyan, LU Hao, CHEN Junmei (School of Material Science and Engineering, Shanghai Jiaotong University, Shanghai 200240, China). p95—98

**Abstract:** By including the increment of transformation strain into the additive decomposition of the increment of total strain, the constitutive model for thermo-mechano-metallurgical analysis was founded. In this model, the behavior of inhomogeneous multiphase mixture was described by using a homogenizing method. On the basis of the model, the welding residual stress in tubular joint of 9Cr1Mo steel was analyzed by using finite element method. In the numerical simulation, a three-dimensional finite element model is used. The calculated results show that the martensitic transition in tubular joint gradually occurs with the movement of welding heating source. As far as the welding residual stress from the three-dimensional analysis is concerned, both the distribution of it in the axial direction of pipeline and the detailed value of it have a good agreement with the experimental results.

**Key words:** thermo-mechano-metallurgical coupled analysis; finite element method; residual stress

**Influence of initial stress of thin pressing parts on welding hot cracking susceptibility** HUANG Yifeng, LU Hao (School of Material Science and Engineering, Shanghai Jiaotong University, Shanghai 200240, China). p99—102

**Abstract:** Thin pressing part has high initial stress level, which affects not only the welding deformation but also hot cracking sensibility. In this paper, initial residual stress of stainless steel pressing part, a CO<sub>2</sub> tank, is measured experimentally. Then it is applied to the welding joint as initial stress in FEM simulation. With re-developed programs, welding process is simulated and analyzed by using thermal elastic-plastic finite element method in software MSC. Marc. The results show that strain in weld zone, radial and circumferential strain in HAZ have few changes by implementing initial axial stress, while total strain and plastic strain in HAZ increase re-

markably. Maximum total stress in the condition with initial stress is more than twice the one without initial stress. So initial axial stress is the main reason of elevated strain level of welding joints, thus increase the hot cracking sensibility.

**Key words:** thin pressing part; initial stress; hot cracking; finite element analysis

**Microstructure and mechanical analysis of Ti-6Al-4V laser butt weld joint** CHENG Donghai, HUANG Jihua, LIN Haifan, ZHANG Hua (College of Materials Science and Engineering, University of Science and Technology Beijing, Beijing 100083, China). p103—106

**Abstract:** Microstructures and mechanical properties of Ti-6Al-4V laser butt weld joints were investigated. The results reveal that the microstructure of laser welded joints consists of coarse columnar crystals. The martensite in columnar crystals crosses like basket shape. Microstructure of HAZ consists of  $\alpha+\beta+\alpha'$ , and distributes non-uniformly, the closer to fusion zone the coarser grains and the more martensite. The suitable welding parameters for 0.8 mm thick Ti-6Al-4V alloy are 1 100—1 300 W and 1.5—3.0 m/min. The mechanical property of weld bead is good, all the tensile specimens fails at base metal away from weld bead, the pattern of fracture shows dimple fracture character.

**Key words:** Ti-6Al-4V alloy; laser welding; microstructure; mechanical properties

**Mechanical property analysis of welding joint made by pulsed submerged arc welding technology** WANG Zhanying<sup>1</sup>, LI Huan<sup>2</sup>, LIANG Jianming<sup>1</sup>, LIN Chundong<sup>1</sup> (1. Department of Mechanical Engineering, Hebei Institute of Architecture and Civil Engineering, Zhangjiakou 075024, Hebei, China; 2. School of Materials Science and Engineering, Tianjin University, Tianjin 300072, China). p107—110

**Abstract:** To solve the disadvantages of mechanical properties of welded joint made by submerged arc welding (SAW) with high heat input, a new pulsed current SAW technology was put forward. The armor plate of 16MnR as the test material was chosen, and the effect of pulsed SAW by using sharp-fall output characteristics power source and varying-speed wire feeder on the mechanical properties of welded joint was investigated. The results of the experiments show that the pulsed arc force can refine the grain size and decrease the composition segregation of deposited metal by regular stirring and oscillating to welding puddle. The microstructures of welded joint by pulsed SAW can be obviously improved and the mechanical properties of welded joint can be increased.

**Key words:** pulse; submerged arc welding; heat input; mechanical property

**Diffusion bonding using powders with a high-content of 2223 phase for superconducting Bi-based tapes** ZOU Guisheng<sup>1</sup>, ZHOU Fangbing<sup>1</sup>, BAI Hailin<sup>1</sup>, WU Aiping<sup>1</sup>, SONG Xiuhua<sup>2</sup> (1. Department of Mechanical Engineering, Tsinghua University, Beijing 100084, China; 2. Beijing Innova Superconductor Technology Co.,